# Electronic Supplementary Information (ESI)

# Rational design and evaluation of the sensing mechanism of a europium(III)-based luminescent turn-ON chemosensor for citrate

Ashwini Kumari Shaw, Nitin Shukla, and Ashis K. Patra*

Department of Chemistry, Indian Institute of Technology Kanpur, Kanpur 208016, Uttar Pradesh, India

E-mail: akpatra@iitk.ac.in

# Table of Contents

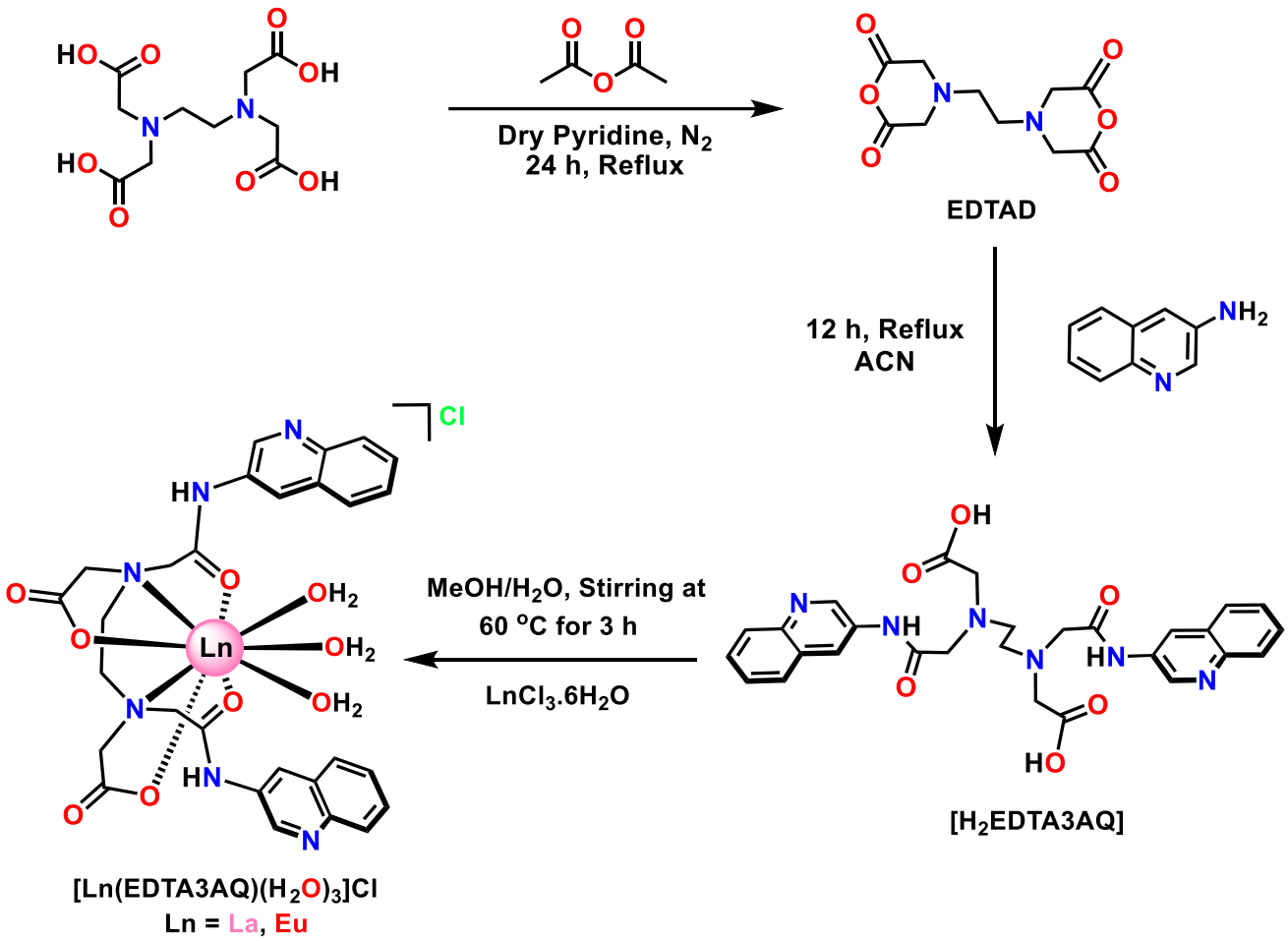


**Figure S1.** General synthesis procedure for the synthesis of $H_2$EDTA3AQ ligand and its lanthanide complexes [Ln(EDTA3AQ)($H_2O$)$_3$]Cl [Ln = Eu (**Eu.1**), La (**La.1**)]

**(a)**

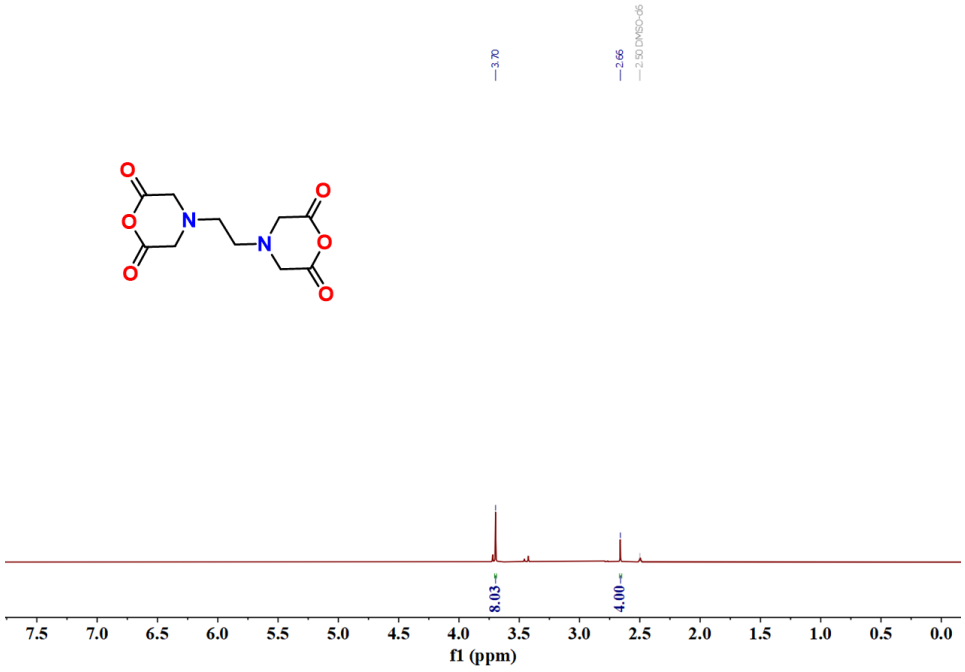


**(b)**

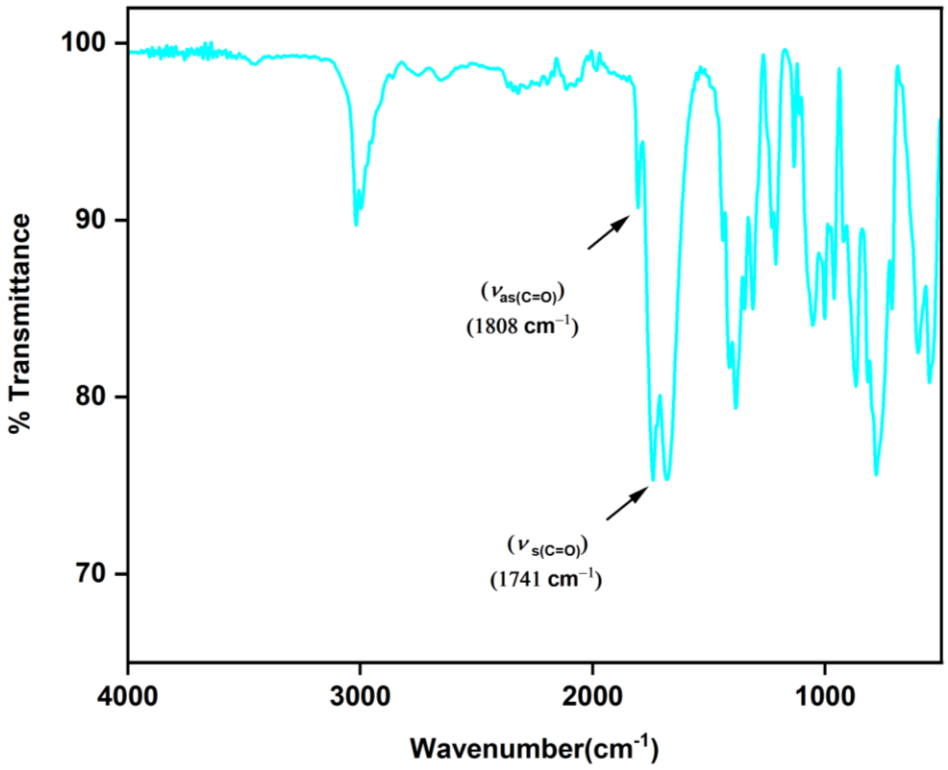


**Figure S2. (a)** $^{1}$H-NMR (400 MHz; DMSO-$d_6$) and **(b)** solid-state FT-IR spectrum of EDTA anhydride (EDAD) at 298 K.

**(a)**

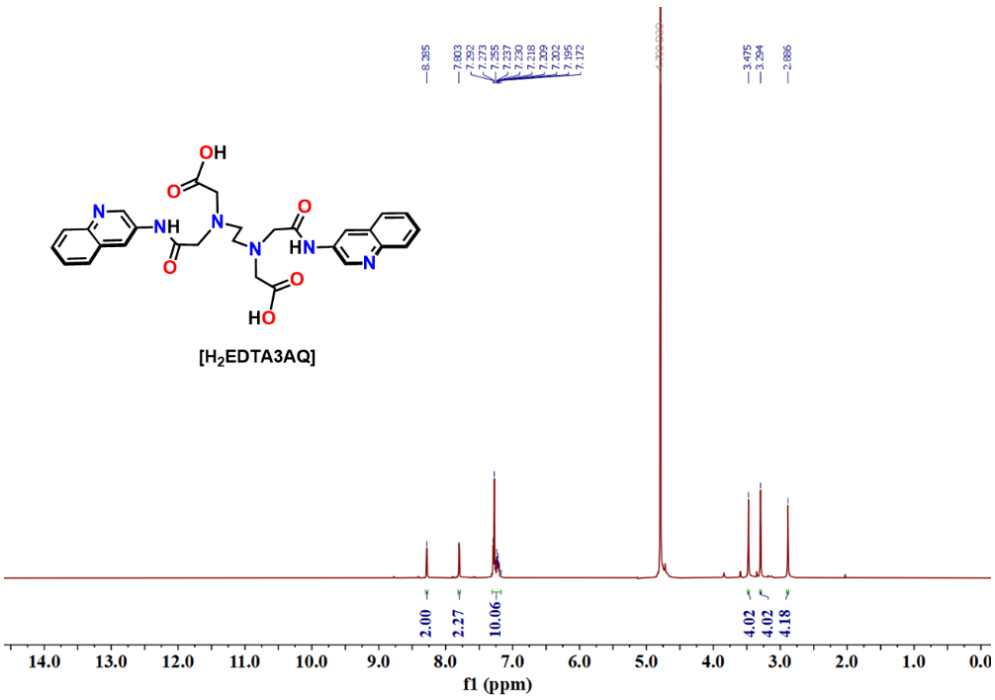


**(b)**

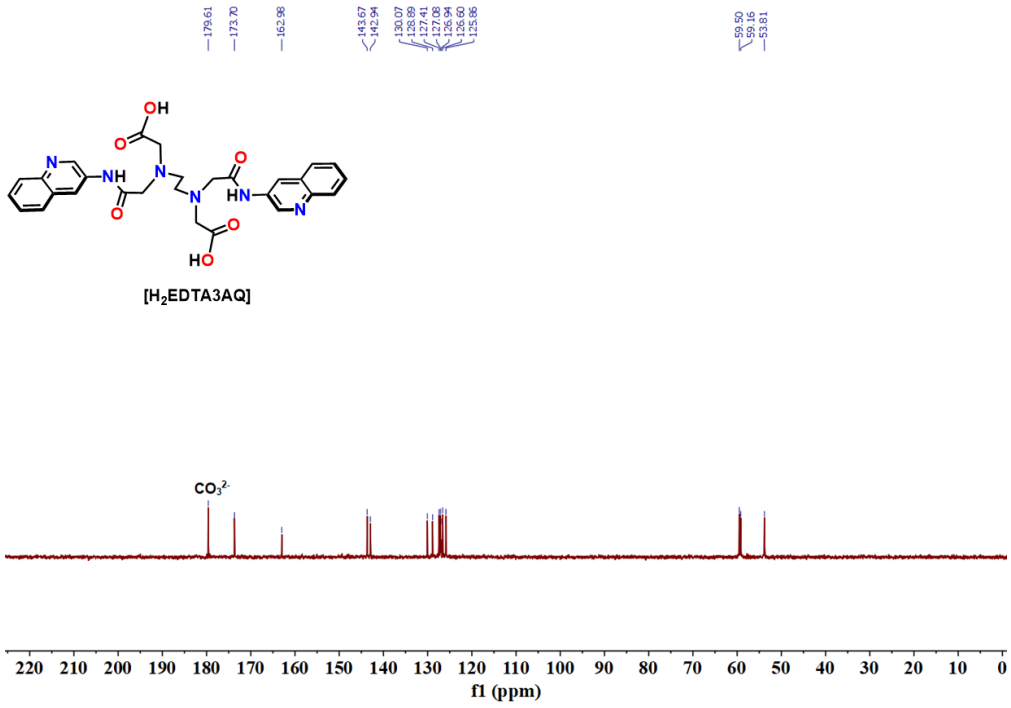


**Figure S3. (a)** $^{1}$H-NMR (400 MHz) and **(b)** $^{13}$C{$^{1}$H}-NMR (101 MHz) spectrum of $H_2$EDTA3AQ in $D_2O$ recorded at 298 K.

**(a)**

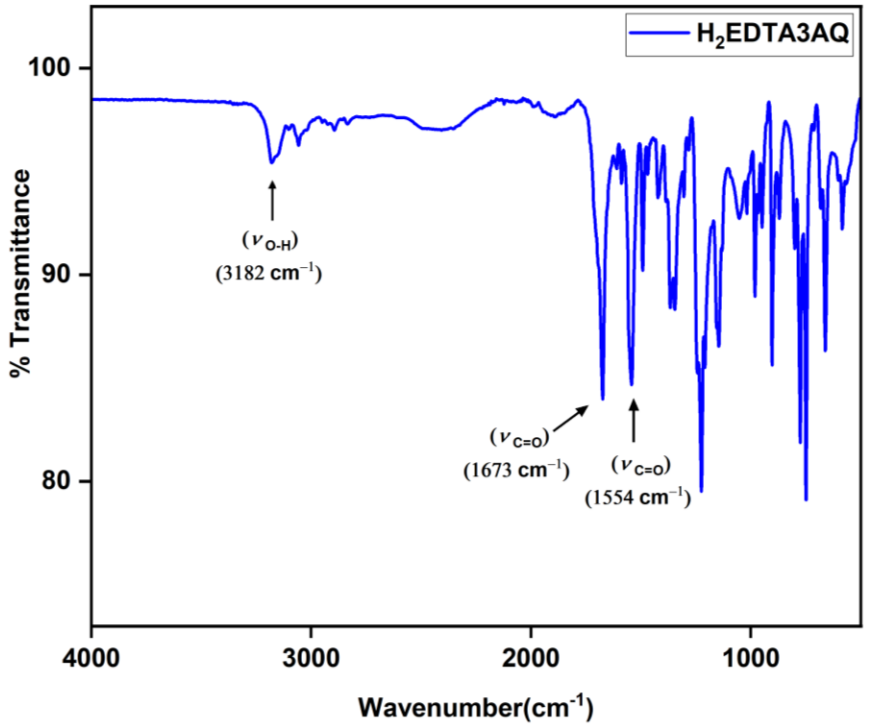


**(b)**

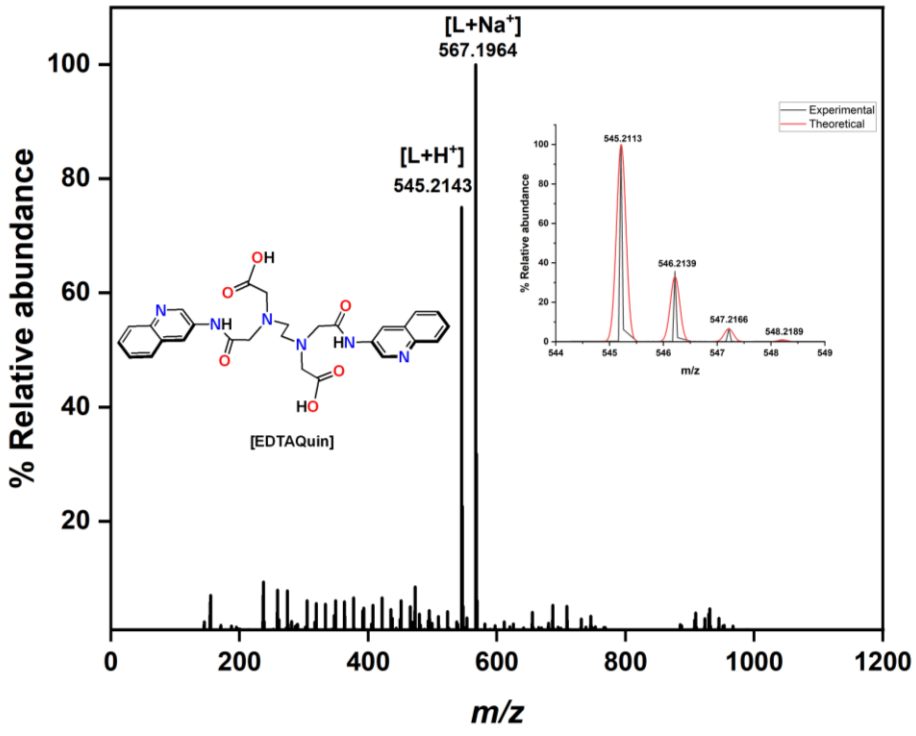


**Figure S4. (a)** Solid-state FT-IR spectra and **(b)** ESI-MS (+ve) spectra of $H_2$EDTA3AQ in DMSO. Overlay of experimental isotopic distribution profile with theoretically calculated *m/z* value of molecular ion peak (*right inset*).

**(a)**

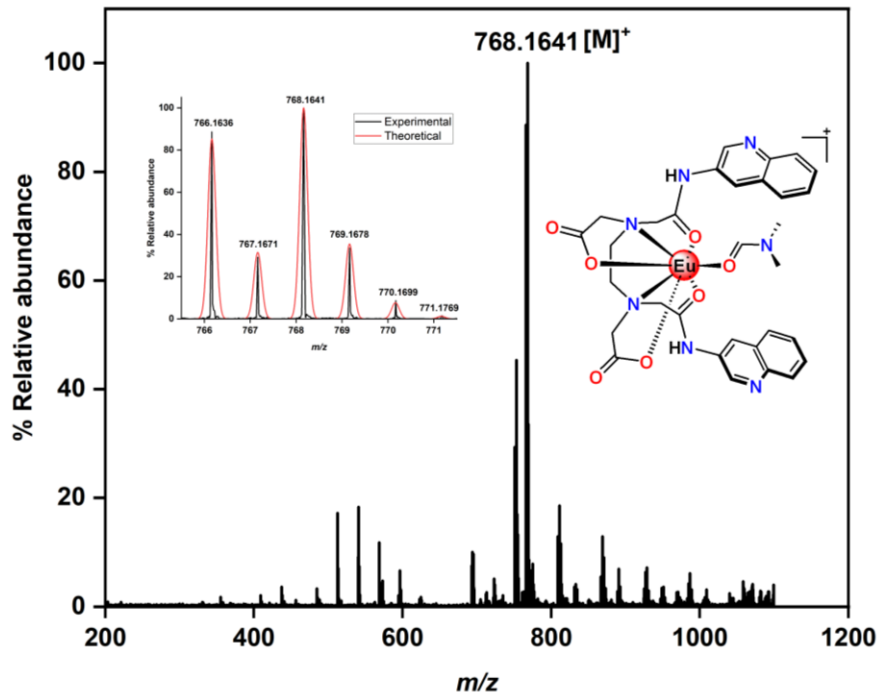


**(b)**

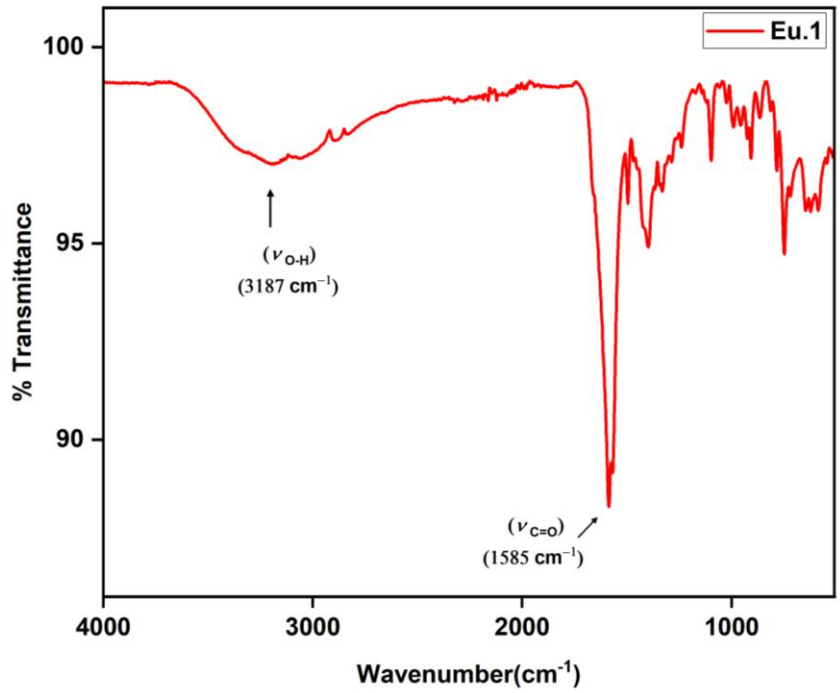


**Figure S5. (a)** ESI-MS (+ve) spectra in DMF and overlay of experimental isotopic distribution profile with theoretically calculated *m/z* value of molecular ion peak (*left inset*). **(b)** Solid-state FT-IR spectra of [**Eu.1**] in KBr phase.

**(a)**

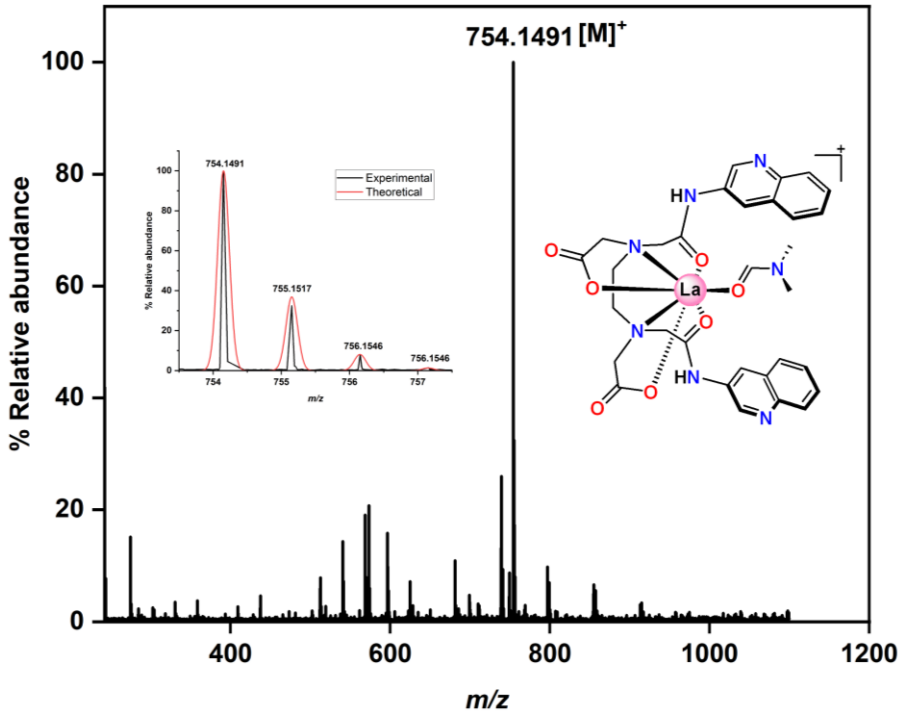


**(b)**

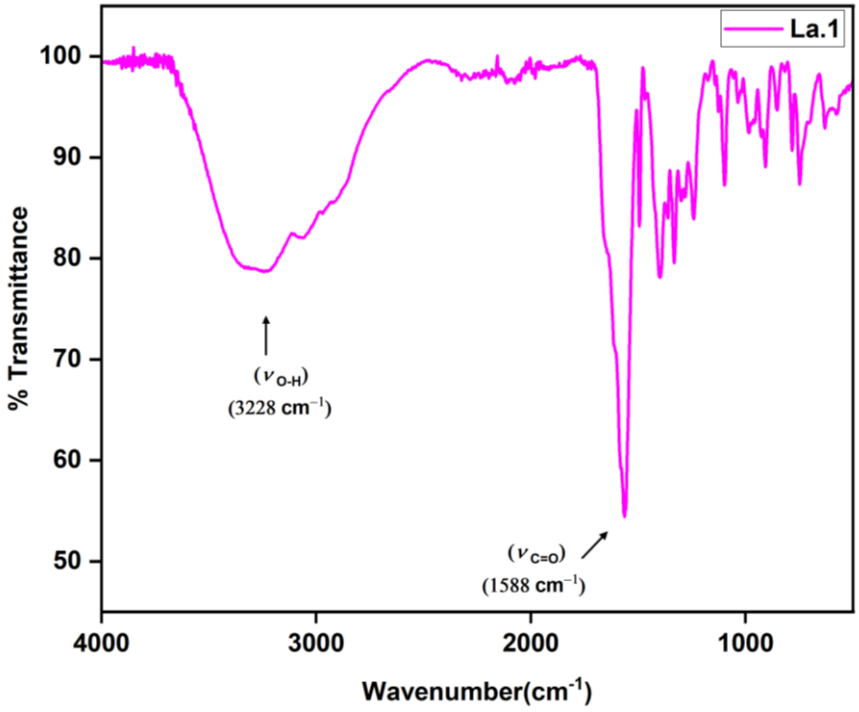


**Figure S6. (a)** ESI-MS (+ve) spectra in DMF and overlay of experimental isotopic distribution profile with theoretically calculated *m/z* value of molecular ion peak (*left inset*). **(b)** Solid-state FT-IR spectra of **[La.1]** in KBr phase.

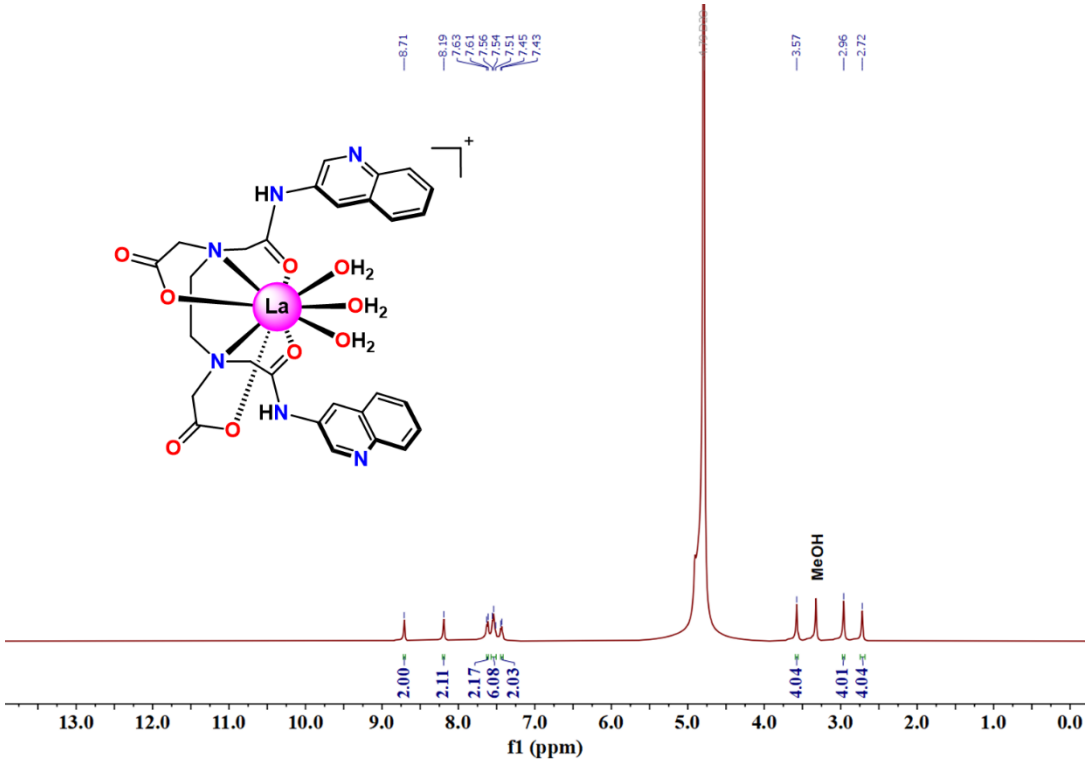


**Figure S7.** $^{1}$H-NMR spectra of [La(EDTA3AQ)($H_2O$)]Cl **(La.1)** in $D_2O$ recorded in a 400 MHz spectrometer at 298 K.

| **Table S1.** Crystallographic data and structure refinement parameters for $H_2$EDTA3AQ ligand | |
|---|---|
| CCDC number | 2488614 (cif: 21octa_0m_a) |
| Identification code | $H_2$EDTA3AQ |
| Empirical formula | $C_{28}H_{28}N_6O_6$ |
| Formula weight | 544.56 |
| Temperature/K | 273.15 |
| Crystal system | monoclinic |
| Space group | $P2_1/n$ |
| $a$/Å | 11.0077(7) |
| $b$/Å | 7.3991(5) |
| $c$/Å | 15.8713(11) |
| $\alpha$/° | 90 |
| $\beta$/° | 106.143(2) |
| $\gamma$/° | 90 |
| Volume/Å$^3$ | 1241.70(14) |
| $Z$ | 2 |
| $\rho_{calc}$ g/cm$^3$ | 1.456 |
| $\mu$/mm$^{-1}$ | 0.105 |
| $F$(000) | 572.0 |
| Crystal size/mm$^3$ | 0.2 × 0.2 × 0.2 |
| Radiation | MoKα ($\lambda$ = 0.71073) |
| 2Θ range for data collection/° | 6.12 to 50.094 |
| Index ranges | $-13 \le h \le 13$, $-8 \le k \le 8$, $-18 \le l \le 18$ |
| Reflections collected | 17658 |
| Independent reflections | 2192 [$R_{int}$ = 0.0581, $R_{sigma}$ = 0.0335] |
| Data/restraints/parameters | 2192/0/183 |
| Goodness-of-fit on F$^2$ | 1.224 |
| Final $R$ indexes [I>=2σ (I)] | $R_1$ = 0.0812, $wR_2$ = 0.1530 |
| Final $R$ indexes [all data] | $R_1$ = 0.0902, $wR_2$ = 0.1570 |
| Largest diff. peak/hole / e Å$^{-3}$ | 0.36/-0.33 |
| $R1 = \Sigma\|\|Fo\|-\|Fc\|\|/\Sigma\|Fo\|$; $wR2 = \{\Sigma[w(Fo^2-Fc^2)^2]/\Sigma[w(Fo^2)^2]\}^{1/2}$. Goodness-of-fit (GOF) $=\{\Sigma[w(Fo^2-Fc^2)^2/(n-p)]\}^{1/2}$, where $n$ = number of data and $p$ = number of parameters refined. | |

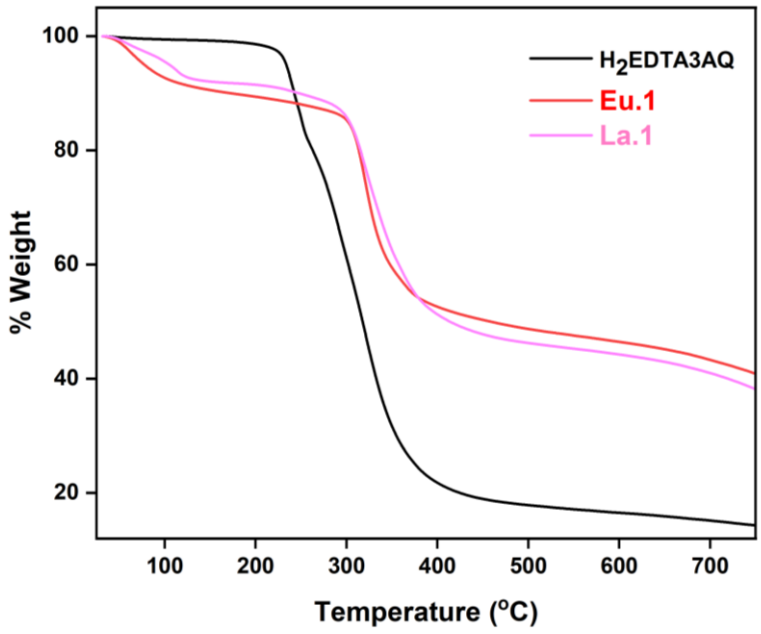


**Figure S8.** TGA plots of complexes EDTA3AQ, **Eu.1, La.1** under a $N_2$ atmosphere with a heating rate of 10 °C $min^{-1}$.

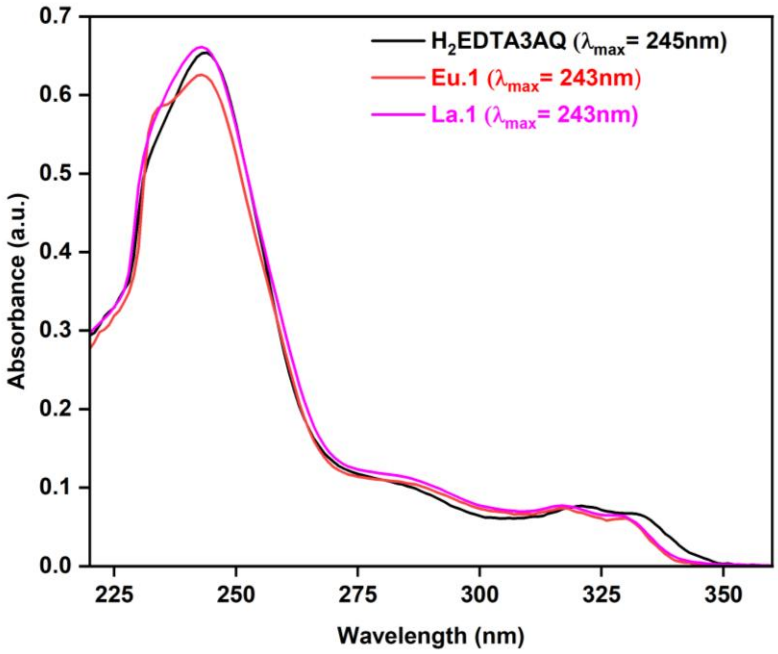


**Figure S9.** UV-Vis absorption spectrum of $H_2$EDTA3AQ ligand (black). $\lambda_{max}$ = 245 nm with a shoulder peak at 321 nm and 332 nm and **[Eu.1]** **(red)**, and **[La.1]** **(magenta)**, $\lambda_{max}$ = 243 nm with a shoulder peak at 317 nm and 330 nm, Conditions: 50 μM in 10 mM HEPES buffer (pH 7.2), $T$ = 298 K.

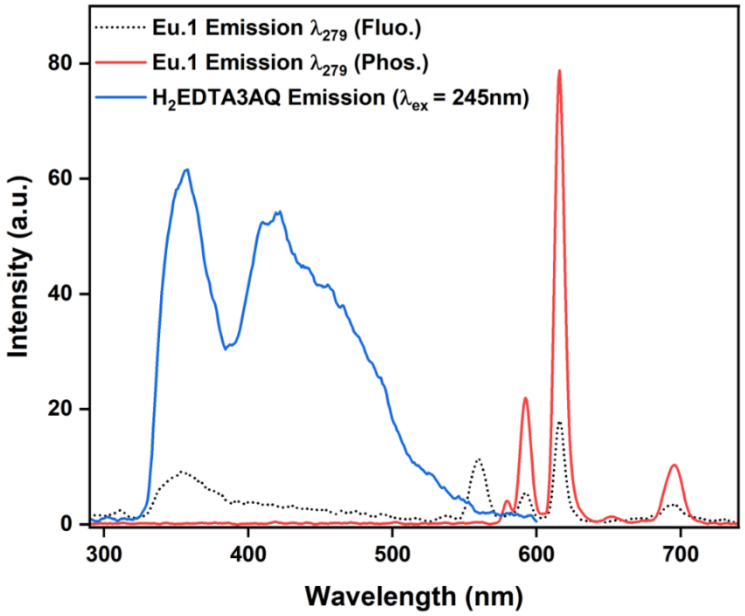


**Figure S10.** Emission spectra of **$H_2$EDTA3AQ** ligand (0.03 mM in DMSO, $\lambda_{ex.}$ = 245 nm) at 298 K. and Steady state fluorescence spectra and time-delayed emission spectra of **Eu.1** (0.03 mM in DMSO, $\lambda_{ex.}$ = 279 nm), delay and gate time = 0.1 ms, $T$ = 298 K, 0.1 M Tris buffer (pH 7.2)].

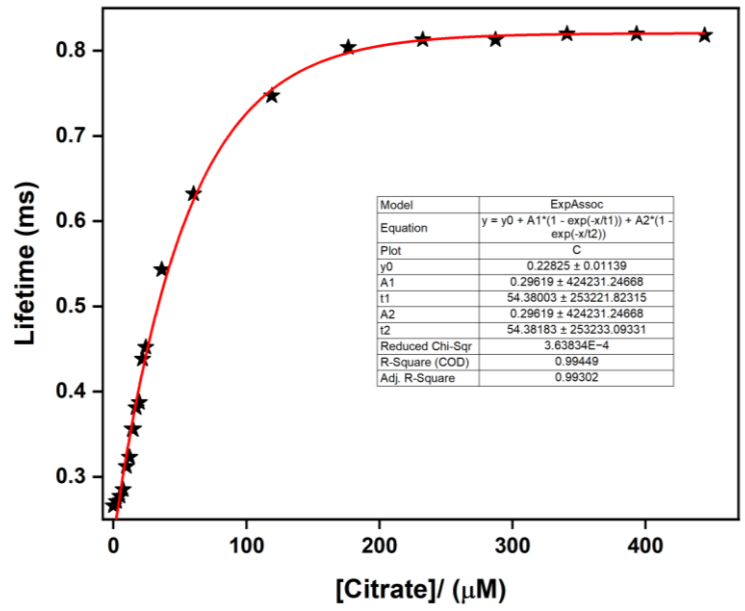


**Figure S11.** Changes in the lifetime of the **Eu.1** probe vs concentration of citrate (μM) added.[$\lambda_{ex.}$ = 330 nm, $\lambda_{em}$ = 616 nm, delay and gate time = 0.5 ms, $T$ = 298 K, Solvent = 10 mM HEPES buffer (pH 7.2)]

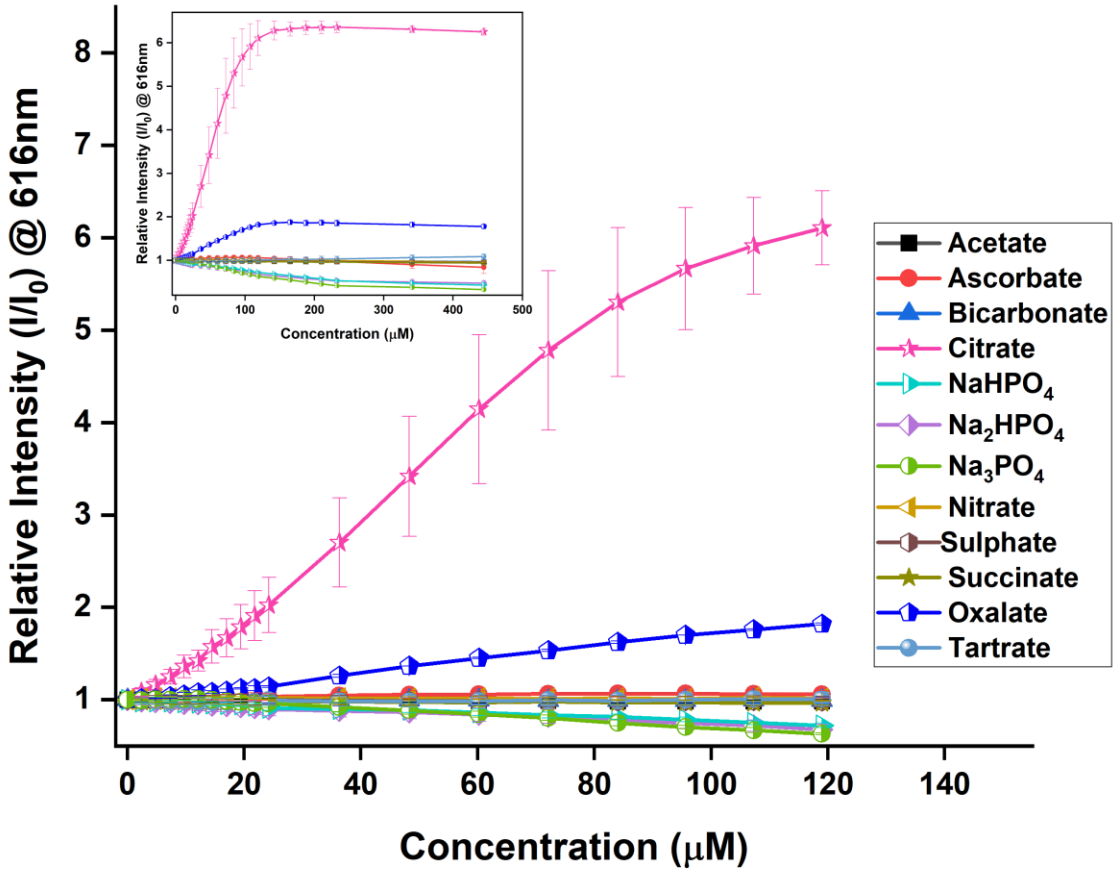


**Figure S12.** Relative changes in emission intensity ($I/I_o$) of the hypersensitive $^5D_0 \rightarrow {}^7F_2$ transition at 616 nm of **Eu.1** in the presence of different analytes. [$\lambda_{ex.}$ = 330 nm, delay and gate time = 0.5 ms, $T$ = 298 K, Solvent = 10 mM HEPES buffer (pH 7.2).]

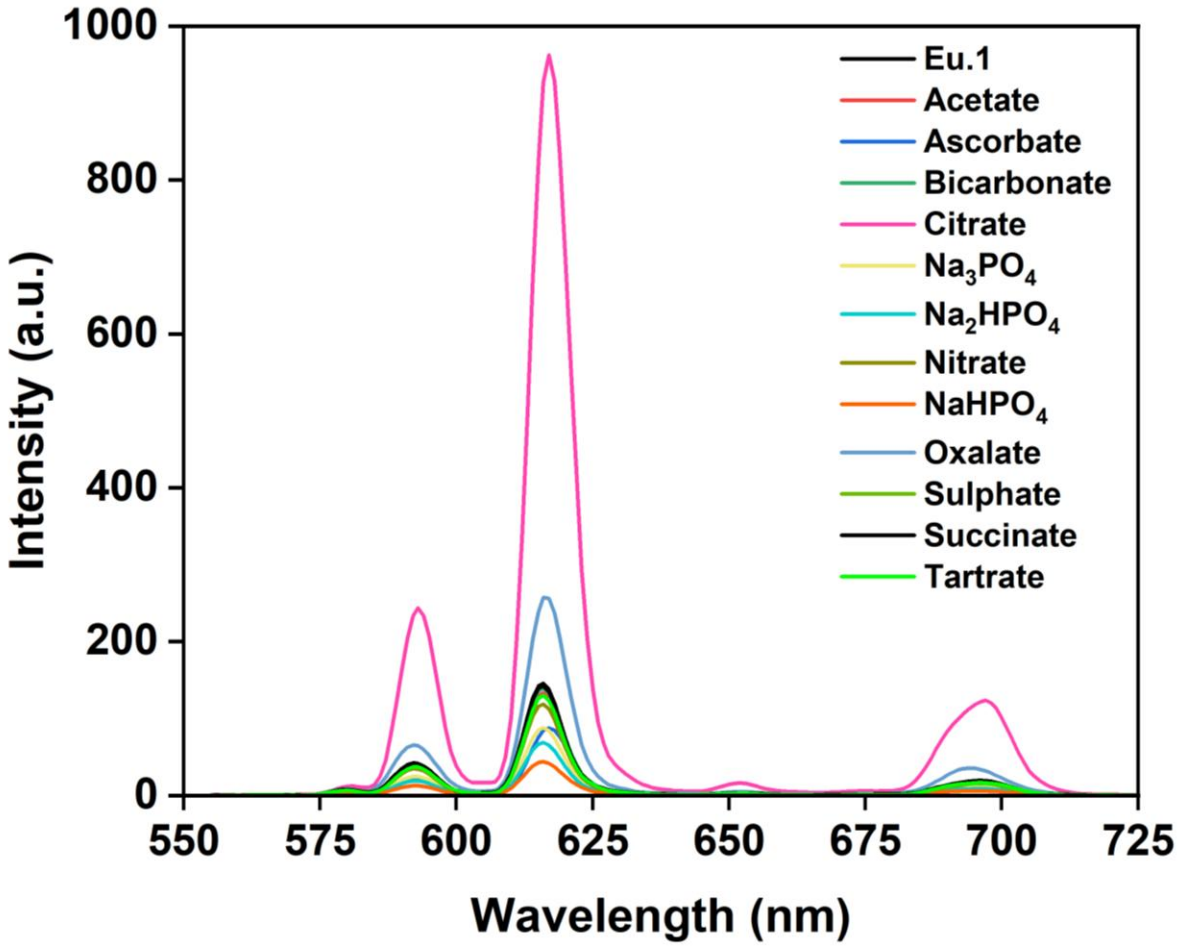


**Figure S13.** Change in time-resolved luminescence (TRL) spectra of **Eu.1** (0.11 mM) (black line) in the presence of 1 equivalent of citrate (pink line) and other interfering anions. [$\lambda_{ex.}$ = 330 nm, delay and gate time = 0.5 ms, $T$ = 298 K, Solvent = 10 mM HEPES buffer (pH 7.2).]

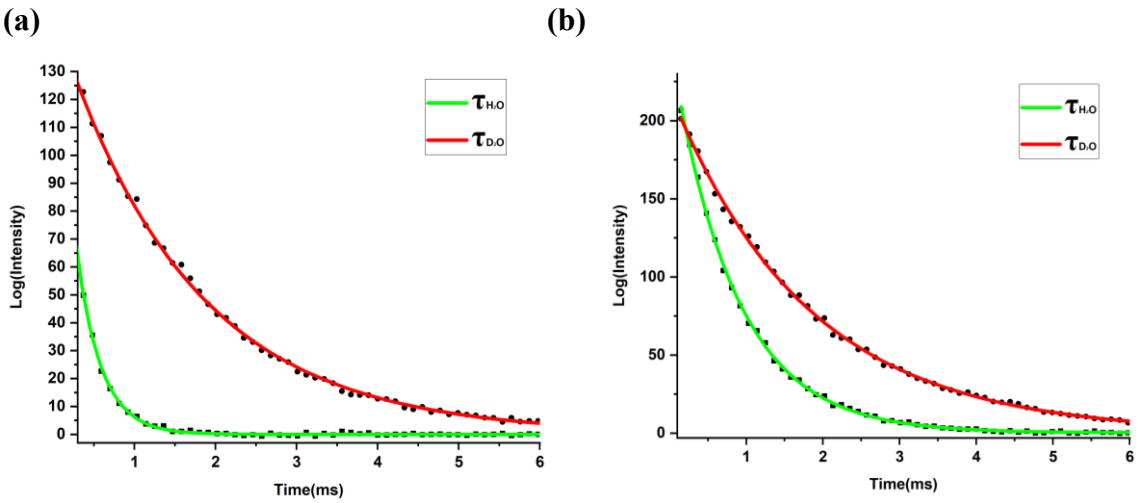


**Figure S14.** Luminescence lifetime of **Eu.1** in $H_2O$ (green) and $D_2O$ (red), in the **(a)** absence and **(b)** presence of citrate. Condition: **[Eu.1] =** 0.11 mM in $H_2O$ and $D_2O$ [$\lambda_{ex.}$ = 330 nm, $\lambda_{em.}$ = 616 nm, ex./em. slit width = 5 nm, delay and gate time = 0.1 ms, $T$ = 298 K.]

**Table S2.** Luminescence lifetime values of **Eu.1** in $H_2O$/ $D_2O$, and calculated $q$ values using Horrock's equation **1**, in the absence and presence of citrate. Condition: **[Eu.1] =** 0.11 mM in $H_2O$ and $D_2O$ [$\lambda_{ex.}$ = 330 nm, $\lambda_{em.}$ = 616 nm, ex./em. slit width = 5 nm, delay and gate time = 0.1 ms, $T$ = 298 K.]

| **Lifetime Analysis** | **Eu.1** | **Eu.1 with citrate** |
|---|---|---|
| $\tau_{H2O}$ **(ms)** | **0.302** | **0.827** |
| $\tau_{D2O}$ **(ms)** | **1.630** | **1.784** |
| **Delay time and gate time** | **0.1 ms** | **0.1 ms** |
| $q$ | **2.93** | **0.37** |

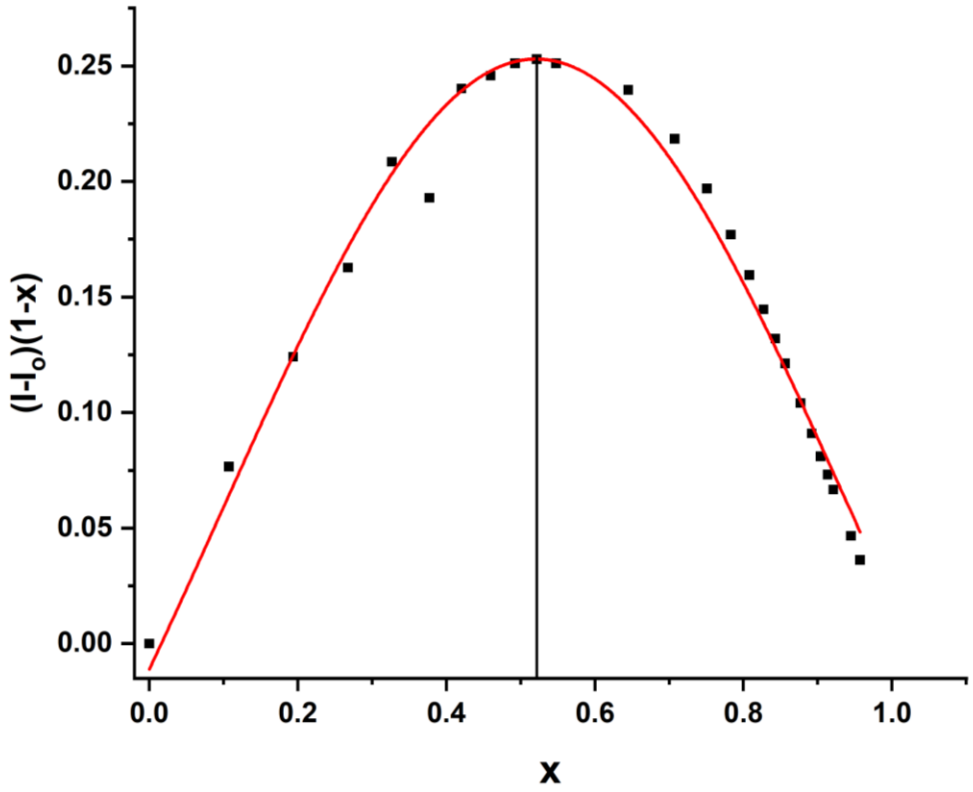


**Figure S15:** Job's plot analysis of **Eu.1** with citrate in 10 mM HEPES buffer (pH 7.2) at $\lambda_{ex}$ = 330 nm, indicating 1:1 adduct formation.

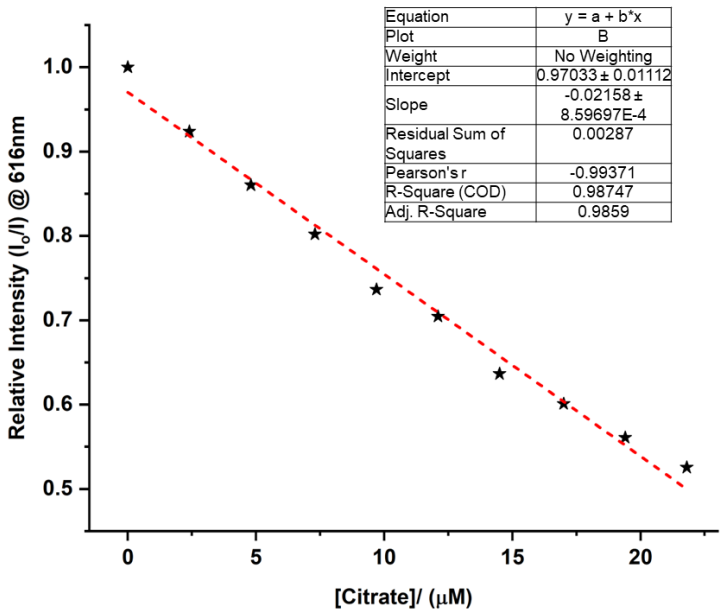


**Figure S16:** . The plot for the calculation of the Limit of Detection (LOD) of Citrate measured from the relative changes in the luminescence intensity at 616 nm ($\Delta J = 2$) upon the gradual increase in concentration of citrate to **Eu.1** (0.11 mM) in 10 mM HEPES buffer (pH 7.2) at $\lambda_{ex}$ = 330 nm, $T$= 298 K.

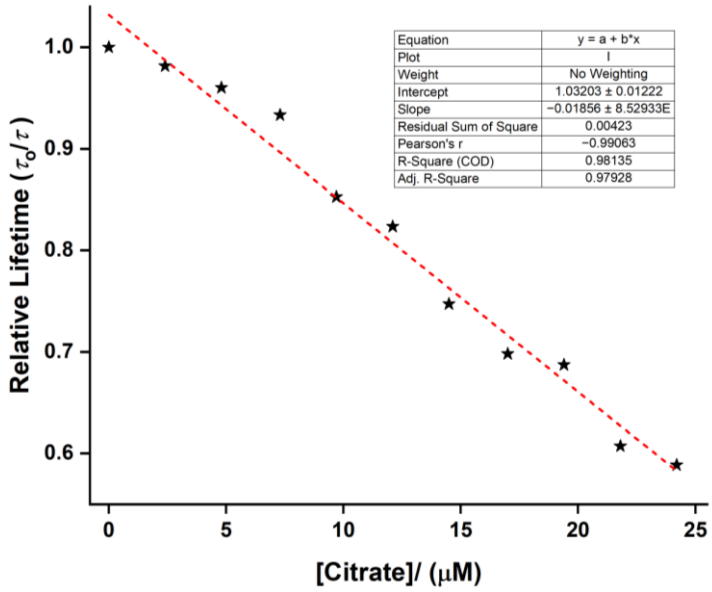


**Figure S17.** The plot for the calculation of the Limit of Detection (LOD) of citrate measured from the relative changes in the lifetime upon gradual increase in concentration of citrate to **Eu.1** (0.11 mM) in 10mM HEPES buffer (pH 7.2) at $\lambda_{ex.}$ = 330 nm, $\lambda_{em}$ = 616 nm, delay and gate time = 0.1 ms, $T$ = 298 K.

**Limit of Detection Calculations:**

$$\boldsymbol{LOD = 3.3\left(\frac{\sigma}{S}\right)} \text{..... (3)}$$

Where $\sigma$ is the standard deviation of the regression line and $s$ is the slope of the curve.

For **Eu.1** vs. citrate titration**:**

| **Table S3.** LOD values of **Eu.1** for citrate using lifetime-based method and intensity-based method in 10 mM HEPES buffer (pH 7.2) at $\lambda_{ex.}$ = 330 nm, $\lambda_{em}$ = 616 nm, $T$ = 298 K. | | |
|---|---|---|
| **Method** | **Lifetime-based** | **Intensity-based** |
| ***s*** | **-0.01856** | **-0.02158** |
| $\sigma$ | **0.01222** | **0.01112** |
| **LOD** | **410 ppb** | **321 ppb** |

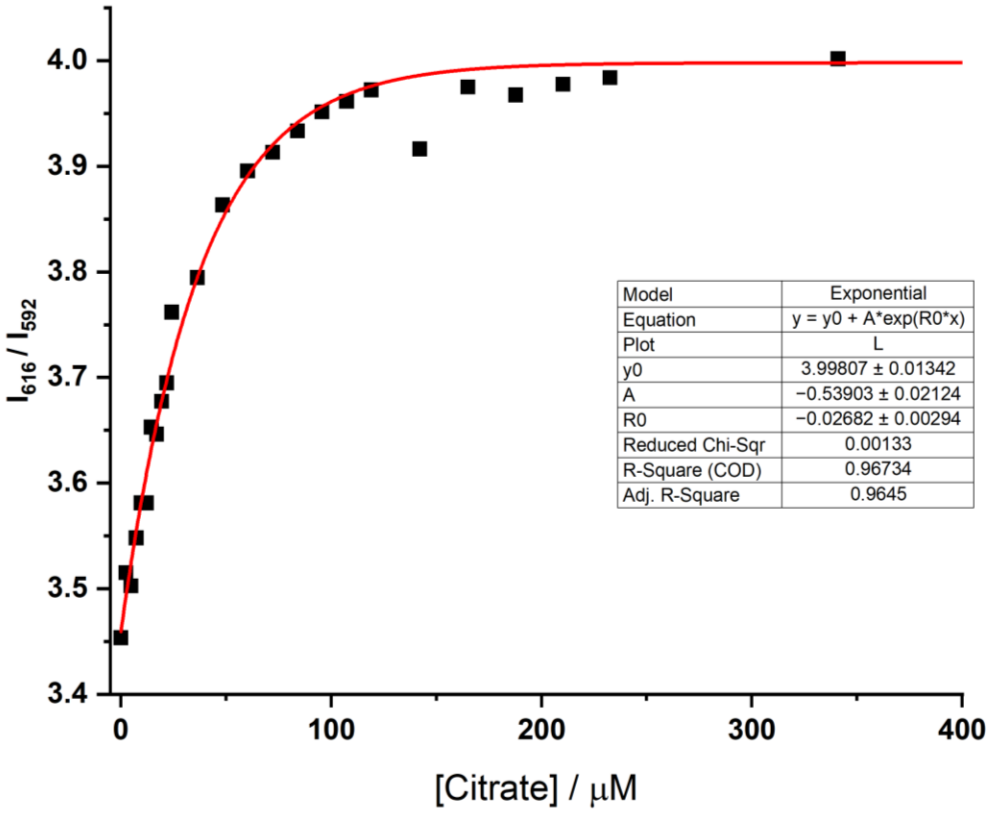


**Figure S18.** Plot for the binding constant (log*Ka*) using the change in the intensity ratio of the $\Delta J = 2/\Delta J = 1$ (616/592 nm) emission bands as a function of citrate concentration in 10 mM HEPES buffer (pH 7.2) at $\lambda_{ex.}$ = 330 nm, $T$= 298 K.

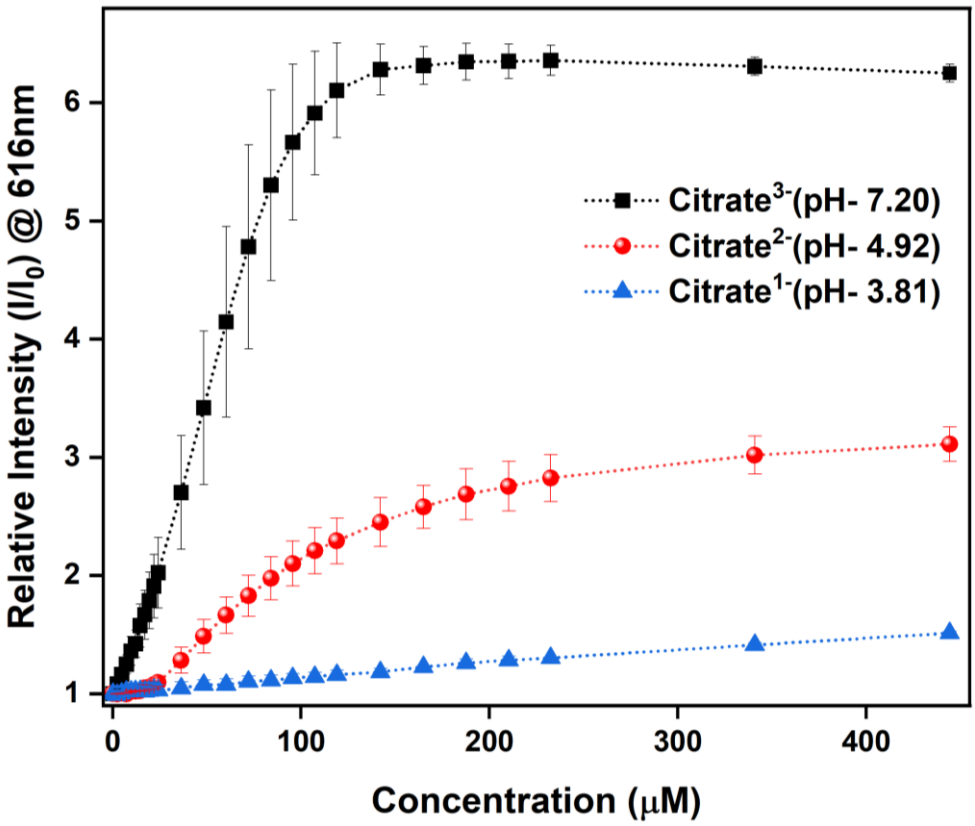


**Figure S19.** Relative changes in emission intensity ($I/I_o$) of the hypersensitive $^5D_0 \rightarrow {}^7F_2$ transition at 616 nm of **Eu.1** in the presence of [citrate]$^{3-}$ (pH 7.20, 10 mM HEPES buffer ), [citrate]$^{2-}$ (pH 4.92, 10 mM Acetate buffer), [citrate]$^{1-}$(pH 3.81, 10 mM Acetate buffer). [$\lambda_{ex.}$ = 330 nm, delay and gate time = 0.5 ms, $T$ = 298 K]

**Calculation for the Radiative ($k_r$) and Non-Radiative ($k_{nr}$) Rate Constants :**

- Radiative rate constant ($k_r$) : $\boldsymbol{k_r = \frac{\phi}{\tau}}$ **..... (4)**
- Non-radiative rate constant ($k_{nr}$) : $\boldsymbol{k_{nr} = \frac{1-\phi}{\tau}}$ **..... (5)**

  Where $\Phi$ = 0.61 %, is the luminescence quantum yield and $\tau$ is the luminescence lifetime of the **Eu.1** probe in $H_2O$.

**Table S4.** Radiative ($k_r$) and non-radiative ($k_{nr}$) rate constants of **Eu.1** probe using eq. 4 and 5, in the absence and presence of citrate [$\lambda_{ex.}$ = 330 nm, $\lambda_{em.}$ = 616 nm, ex./em. slit width = 5 nm, delay and gate time = 0.1 ms, $T$ = 298 K.]

| **Rate Constant Analysis** | $\tau$ **(ms)** | $k_r$**(s$^{-1}$)** | $k_{nr}$**(s$^{-1}$)** |
|---|---|---|---|
| **Eu.1** | **0.302** | **$0.02\times10^{-3}$** | **$3.29\times10^{-3}$** |
| **Eu.1 + Citrate** | **0.827** | **$0.0074\times10^{-3}$** | **$1.20\times10^{-3}$** |

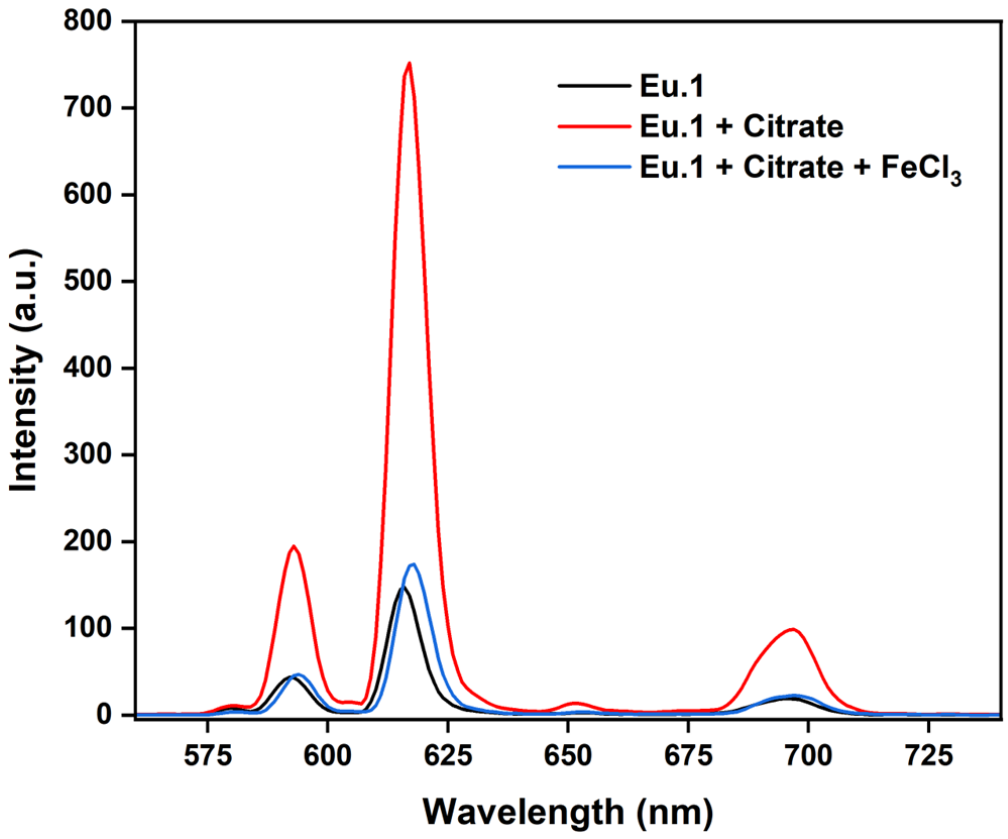


**Figure S20**. Change in emission spectra of **Eu.1** (0.11 mM, black line) in the presence of citrate (red line) and recovery of **Eu.1** probe upon sequestration of citrate using $FeCl_3$ (blue line). [$\lambda_{ex.}$ = 330 nm, delay and gate time = 0.5 ms, $T$ = 298 K, Solvent = 10 mM HEPES buffer (pH 7.2)]s